

Self-Organized Criticality in Nonconserved Systems

A. Alan Middleton and Chao Tang

NEC Research Institute, 4 Independence Way, Princeton, New Jersey 08540

(Received 23 June 1994)

The origin of self-organized criticality in a model without conservation law [Z. Olami, H. Feder, and K. Christensen, *Phys. Rev. Lett.* **68**, 1244 (1992)] is studied. The initially periodic and neutrally stable interior of the system is invaded by a “self-organized” region. This self-organization is due to the synchronization of the individual elements with each other. A simplified model of marginal oscillator locking on a directed lattice explains many of the features in the nonconserved model: in particular, the dependence of the avalanche-distribution exponent on the conservation parameter α is examined.

PACS numbers: 64.60.-i, 05.45.+b, 05.70.Jk, 91.30.-f

The phenomenon of the self-organized criticality (SOC) [1] is characterized by spontaneous and dynamical generation of scale invariance in an extended nonequilibrium system. One of the key issues in this field is to identify the mechanism(s) of SOC. It has been conjectured that conservation laws or special symmetries are necessary [2]. Conservation laws certainly are of great importance in “sandpile” models [1,3,4], where the scale invariance can be shown to follow from a local conservation law [5]. In this sense, the origins of long-range correlations in SOC systems with conservation are well understood, though not all exponents have been calculated analytically. However, models have been constructed [6–11] that have no apparent conservation law, and yet display a power-law distribution of avalanche sizes. Of particular interest is the model proposed by Olami, Feder, and Christensen (OFC) [9,12,13] which, they argue, models earthquake dynamics. In this paper, we study in detail the OFC model and we find that the self-organization is due to synchronization or “phase locking”—a mechanism very different from that in the conserved models.

In the OFC model, dynamical “height” variables h_i are defined on sites i of a square lattice. The h_i increase at unit rate until $h = 1$ at some location. The site j where $h_j = 1$ is considered to be unstable and will “topple.” The rule of toppling is that when $h_j \geq 1$, then $h_k \rightarrow h_k + \alpha h_j$, for all k neighboring j , and $h_j \rightarrow 0$. The toppling on site j may cause its neighbors to become unstable ($h_k \geq 1$) and to topple [14]. This procedure is repeated until all sites are stable ($h_i < 1$ everywhere). The magnitude of the avalanche is given by the total “energy” dissipated in the process, i.e., the total change in $\sum_i h_i$. The avalanche, which happens instantly on the time scale of driving [15], is then followed by growth. The parameter α is the measure of conservation (of h 's). When $\alpha = 1/4$, the model is conserved and it is in the same universality class as for the Bak-Tang-Wiesenfeld model [1,9,16]. We study here the nonconservative case $0 < \alpha < 1/4$.

We find that the system with periodic boundary conditions quickly reaches an exactly periodic state [12], with a unique period in the slow time. It has been noted

[9,13] that in the case of periodic boundary conditions, the avalanche size distribution function drops very quickly with size. In the case of our modified model, which prevents two sites from having the same value of h , all avalanches consist of the toppling of exactly one lattice site, after a brief transient time. In a periodic state, the h_i 's take turns to topple, one by one. The height h decreases by one each time a site topples and increases by 4α due to the toppling of the four neighbors when they reach $h = 1$. Thus the period of all these periodic states is $1 - 4\alpha$ in the slow time variable t , so that the slow “growth” is balanced exactly by the dissipation due to toppling. These periodic states are highly degenerate and neutrally stable in the sense that a typical small perturbation of the height at a single site in a periodic state is still a periodic state. They are similar to the neutrally stable periodic states in coupled oscillators [17]. There is a continuous set of periodic states in the attractor, with measure $(1 - 4\alpha)^V$ in the initial phase space, where V is the system volume.

Any inhomogeneity, such as a change in boundary conditions, destroys such simple periodic states. When the boundary conditions are open, the system can no longer have period $1 - 4\alpha$, as the boundary sites have three neighbors (we study a system that is open on one axis, with the other directions periodic). Initially, the interior sites quickly converge to a nearly periodic state and topple with period $1 - 4\alpha$, but the boundaries are aperiodic. At longer times, the aperiodic region invades the periodic interior, as shown in Fig. 1. This invasion, which destroys the periodicity in the interior and builds up long-range correlations, occurs by a mechanism similar to oscillator locking, as we describe below. The interface between the two regions is well defined on scales larger than a lattice constant. The invasion distance appears to have a power-law dependence on time, $y(t) \sim t^{\beta(\alpha)}$ as shown in Fig. 2, with $\beta = 0.23 \pm 0.08, 0.63 \pm 0.08$ for $\alpha = 0.07, 0.15$, respectively. We see such invasion occurring even for values of $\alpha < 0.05$, though β appears to be quite small, so that the invasion is extremely slow. This suggests that the transition to non-SOC behavior

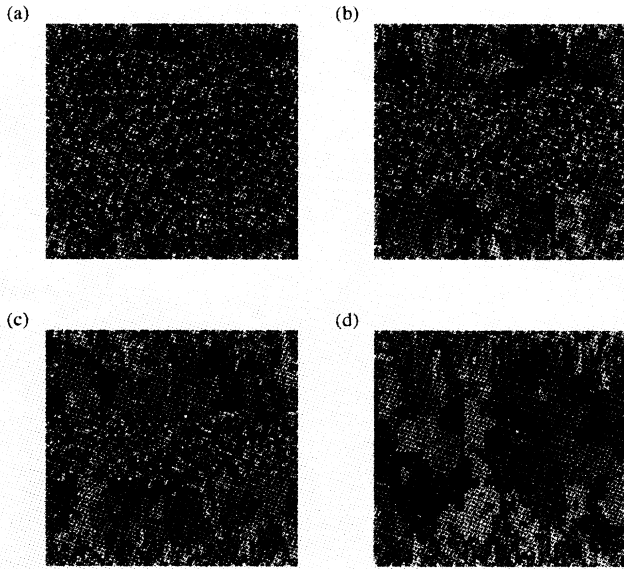


FIG. 1. Configurations of the Olami-Feder-Christensen model at various times after random initialization, demonstrating the invasion of the short-range correlated interior by the ‘‘SOC region.’’ The color corresponds to the height variables $0 \leq h_i < 1$. The boundaries are periodic in the vertical direction and open in the horizontal. The lattice consists of 64^2 sites, with $\alpha = 0.07$. Times are $t =$ (a) 1.2×10^3 , (b) 2.4×10^3 , (c) 6.0×10^3 , and (d) 36.0×10^3 .

claimed by Olami, Feder, and Christensen [9] may only be apparent, due to the finite time of the simulations; we note that the time for complete invasion of a 128^2 system with $\alpha = 0.07$ is greater than 10^{10} avalanches. In the limit of long times, when the invasion crosses the whole sample,

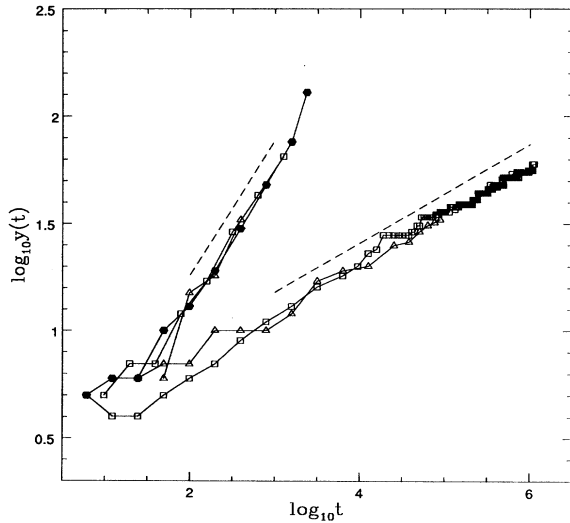


FIG. 2. A plot of the invasion distance vs time for conservation parameters $\alpha = 0.07, 0.15$. Power-law fits are shown as dashed lines; symbols indicate system size ($\Delta = 64^2$, $\square = 128^2$, and $\bullet = 256^2$).

the distribution $P(s; \alpha)$ of avalanches of size s is a power law, with

$$P(s; \alpha) \sim s^{-\tau(\alpha)}. \tag{1}$$

Consistent with OFC, we find $\tau(\alpha) = 3.2 \pm 0.1, 2.3 \pm 0.1$ for $\alpha = 0.07, 0.15$, respectively. The avalanches are not uniformly distributed in the system; the typical avalanche size grows with distance from the edge [18].

The spatial distribution of length scales is apparent in Fig. 1(d), which shows an example of a configuration between avalanches in the steady state. Near the boundaries, the h_i have only short-range correlations, but this correlation length grows with distance from the boundary. We define a toppling rate $r(y)$ as a function of distance y from the boundary, which gives the inverse of the mean time between topplings. At the boundaries, where the sites have only three neighbors, $r(y)$ is smaller than the interior, where $r(y) \rightarrow (1 - 4\alpha)^{-1}$ as $y \rightarrow \infty$. The toppling rate differential, defined as $\delta r(y) = (1 - 4\alpha)^{-1} - r(y)$, is found to behave as

$$\delta r(y) \sim y^{-\eta}, \tag{2}$$

with $\eta = 3.2 \pm 0.6, 1.8 \pm 0.2$ for $\alpha = 0.07, 0.15$, respectively. Let $h_t(y)$ be the average height just before toppling, $R(y) \equiv (1 - 4\alpha)r(y)h_t(y)$ is then the dissipation rate and $R(y) \rightarrow 1$ as $y \rightarrow \infty$. It can be shown that in the steady state $\delta R(y) = 1 - R(y)$ behaves as $\delta R(y) = \exp\{-y[(1 - 4\alpha)/\alpha]^{1/2}\}$. Thus the dissipation rate is rather uniform except within a boundary layer of thickness $[\alpha/(1 - 4\alpha)]^{1/2}$. The power-law behavior of Eq. (2) must be compensated by a power law in $\delta h_t(y) = h_t(y) - 1$:

$$\delta h_t(y) \sim y^{-\eta}. \tag{3}$$

In order to gain some insights on the buildup of long-range correlations in the inhomogeneous system, we consider a system which has only two sites: h_1 and h_2 . Let us first consider the homogeneous case: both h_1 and h_2 are driven with unit rate and when one of them reaches the value one it topples. The rule of toppling is that if $h_{1(2)} \geq 1$, then $h_{2(1)} \rightarrow h_{2(1)} + \alpha h_{1(2)}$ and $h_{1(2)} \rightarrow 0$. This small system has a continuous set of periodic states which are marginally stable. To illustrate its dynamics, we construct a Poincaré map. Denote $h_1(n)$ to be the value of h_1 right after the n th toppling of h_2 . It is easy to show that [12]

$$h_1(n + 1) = \begin{cases} h_1(n), & \alpha \leq h_1(n) < 1, \\ 1 + \alpha - \alpha h_1(n), & 1 \leq h_1(n) < 1/\alpha, \\ \alpha^2 h_1(n), & h_1(n) \geq 1/\alpha, \end{cases} \tag{4}$$

which is sketched in Fig. 3(a). We see that there is a line of marginally stable fixed points $h_1^* \in [\alpha, 1)$. These fixed points are periodic states with period $1 - \alpha$: h_1 and h_2 take turns to topple and the toppling of one site will not trigger the toppling of another ($h_1^* < 1$). Now, we introduce a small inhomogeneity. We drive h_1 with rate 1,

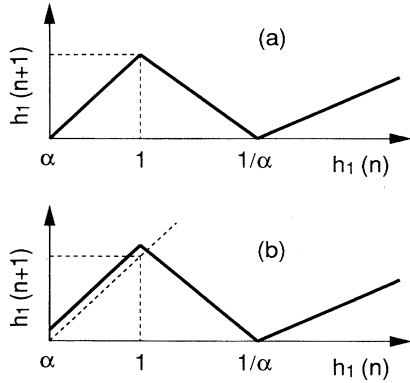


FIG. 3. Return map for the two-site system: (a) homogeneous system; (b) inhomogeneous system.

but h_2 with a slightly slower rate $(1 + \epsilon)^{-1}$. The Poincaré map now reads

$$h_1(n + 1) = \begin{cases} h_1(n) + \epsilon(1 - \alpha), & \alpha \leq h_1(n) < 1, \\ 1 + \alpha + \epsilon - \alpha(1 + \epsilon)h_1(n), & 1 \leq h_1(n) < 1/\alpha, \\ \alpha^2 h_1(n), & h_1(n) \geq 1/\alpha, \end{cases} \quad (5)$$

which is sketched in Fig. 3(b). In this case, there is only one fixed point $h_1^* = 1 + \epsilon(1 - \alpha)/(1 + \alpha)$. This fixed point is the phase-locked or synchronized state: the toppling of h_2 will trigger h_1 to topple ($h_1^* > 1$). Note that Eq. (5) is only ϵ away from Eq. (4), so the locking is rather weak and fluctuations can play a crucial role. In the OFC model with open boundary conditions, the boundaries introduce inhomogeneity. The sites at the open boundaries have only three neighbors and hence have a *slower effective growth rate*. This inhomogeneity in the effective growth rate propagates into the interior of the sample, causing phase locking and thus long-range correlation. However, the whole system is not in a synchronized state. Rather, it is only “marginally” locked so that it gives a power-law distribution of avalanche sizes.

We do not have a complete theory for the emergence of the “marginal locking” in the OFC model. However, we can abstract some of the features to construct a simpler model which also exhibits SOC. This model is defined on a directed lattice to simplify avalanches. We define dynamical variables $0 \leq \phi_i < 1$ as the *phase* of the next toppling time of a site; this phase is related to the height h_i in the OFC model at a fixed time. At random sites on the boundary, we initiate a toppling which changes the phase according to $\phi_i \rightarrow \phi'_i = \phi_i + \alpha$. If the phase ϕ_j at a neighboring “downhill” site $j = i + \hat{x}$ or $i + \hat{y}$ (see inset in Fig. 4) meets the locking condition $(\phi_i - \phi_j \bmod 1) < \alpha$, the site j locks onto the boundary site, with $\phi_j \rightarrow \phi'_j$. This disturbance can then continue to propagate by sites further from the boundary, becoming locked in zero time. We refer to this locking as marginal since neighboring phases only lock upon a *crossing* in the toppling time;

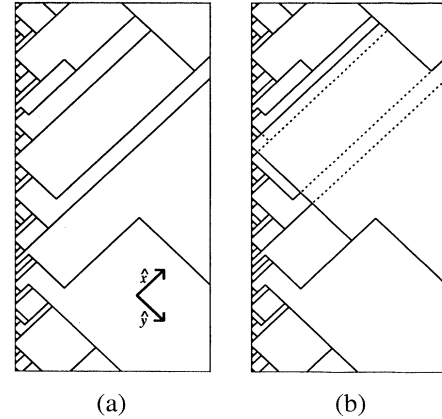


FIG. 4. Domains in the simplified SOC model described in the text, for a 200^2 directed lattice. (a) Configuration with domains of identical toppling times indicated by solid lines. (b) Configuration after an avalanche, with previous domains indicated by dashed lines. The inset sketches the directed lattice.

the configuration is neutrally stable with respect to a continuous set of perturbations. This model differs from the OFC model most notably in the directed lattice and the instantaneous locking (avalanches in OFC occur in zero time, but locking occurs over a period of time).

A snapshot of the ϕ_i in the steady state is depicted in Fig. 4(a). The domains, bounded by solid lines, are regions where the toppling times are identical. Figure 4(b) shows a configuration after an avalanche, with the dotted lines showing the previous domain configuration. An avalanche crosses domain boundaries only when the neighboring domains have times that differ by no more than α . Numerically, it is found that the number of domains $n(d)$ of size d at a fixed time has a power-law tail that is independent of α , $n(d) \sim d^{-\sigma}$, with $\sigma = 1.495 \pm 0.005$. Yet the avalanche distribution has an α -dependent exponent, with the probability of an avalanche of size s behaving as $P(s) \sim s^{-\tau(\alpha)}$ (Fig. 5). Note that domains and avalanches are closely related, with avalanches defining domains. The exponent σ must satisfy the bound $\sigma \leq 3/2$; the fact that our numerical result saturates this inequality, to within numerical error, suggests that the average width of a domain is proportional to the length of the domain perpendicular to the boundary.

The α -dependent relationship between τ and σ can be approximately explained. Assuming that the toppling times of neighboring domains are independent variables, the probability of an avalanche, which starts in one domain, incorporating a given neighboring domain (i.e., crossing the domain boundary) is just α . The incorporation of a neighboring domain increases the avalanche size to the scale of the neighboring domain, typically larger than the scale of the original domain. Assuming a scale independent probability $\alpha' \propto \alpha$ that the *avalanche does not stop at a domain wall*, the avalanche distribu-

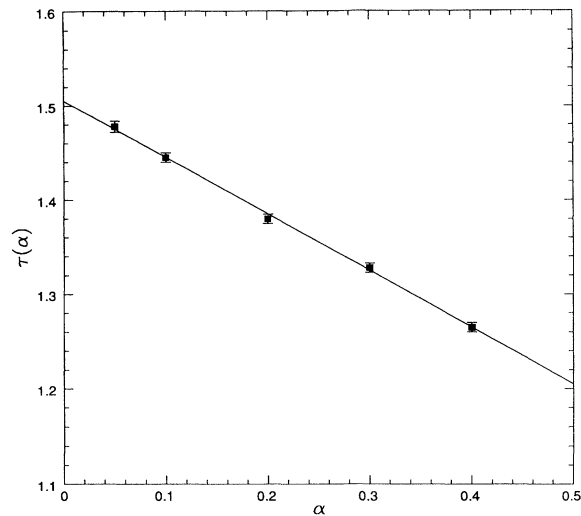


FIG. 5. The avalanche distribution exponent $\tau(\alpha)$ for the directed model as a function of the conservation parameter α . The linear fit is discussed in the text.

tion is broader than the domain distribution and is α dependent. This can be seen by considering the distribution of the logarithm of the avalanche sizes $N_s(\ln s)$. The distribution of the logarithm of domain sizes behaves as $N_d(\ln d) \sim \exp[-(\sigma - 1) \ln d]$. An avalanche terminates when the edge of a domain is reached, which happens at “rate” $\sigma - 1$, considering $\ln s$ as time, and the avalanche is stopped at this edge, which happens with probability $1 - \alpha'$. The total avalanche termination rate as $\ln s$ increases is $(\sigma - 1)(1 - \alpha')$, giving $N_s(\ln s) \sim \exp[-(\sigma - 1)(1 - \alpha') \ln s]$. This results in the avalanche distribution $P(s) \sim s^{-\tau(\alpha)}$, with $\tau(\alpha) = \sigma - \alpha'(\sigma - 1)$. This is in agreement with the linear fit of Fig. 5, with $\alpha' = (1.20 \pm 0.04)\alpha$; the fitted value of $\tau(0) = \sigma = 1.505 \pm 0.005$ agrees with the value determined by the domain distribution.

In this paper we have examined how SOC can arise in a model without a conservation law. The OFC model with periodic boundary conditions has a continuous set of neutrally stable periodic states. In general, inhomogeneity destroys these periodic states and causes phase locking which is the building block for long-range correlations. We found that an open boundary results in the invasion of the interior by a marginally locked region in which the avalanche size distribution is a power law. A simplified model on a directed lattice has been used to demonstrate how an α -dependent avalanche size distribution exponent can arise in such nonconserved dynamical models. We note that the OFC model is similar to the coupled “integrate-and-fire” oscillators studied in the context of neural networks and biology. A close cousin is Peskin’s model for the cardiac pacemaker [19]. We found that the model in 2D with nearest neighbor cou-

pling tends to lock into some periodic or “quasiperiodic” cluster state and that it has richer behaviors than simple synchronization. It would be interesting to further investigate the relationship between the OFC model and neural network models.

-
- [1] P. Bak, C. Tang, and K. Wiesenfeld, Phys. Rev. Lett. **59**, 381 (1987); Phys. Rev. A **38**, 364 (1988).
 - [2] G. Grinstein, D.-H. Lee, and S. Sachdev, Phys. Rev. Lett. **64**, 1927 (1990).
 - [3] L. Kadanoff, S. Nagel, L. Wu, and S. Zhou, Phys. Rev. A **39**, 6524 (1989); A. Chhabra, M. Feigenbaum, L. Kadanoff, A. Kolan, and I. Procaccia, Phys. Rev. E **47**, 3099 (1993).
 - [4] J. Carlson, J. Chayes, E. Grannan, and G. Swindle, Phys. Rev. Lett. **65**, 2547 (1990).
 - [5] S. Majumdar and D. Dhar, Physica (Amsterdam) **185A**, 129 (1992).
 - [6] P. Bak, K. Chen, and M. Creutz, Nature (London) **342**, 780 (1989).
 - [7] H. Feder and J. Feder, Phys. Rev. Lett. **66**, 2669 (1991).
 - [8] B. Drossel and F. Schwabl, Phys. Rev. Lett. **69**, 1629 (1992); C. Henley, Phys. Rev. Lett. **71**, 2741 (1993).
 - [9] Z. Olami, H. J. S. Feder, and K. Christensen, Phys. Rev. Lett. **68**, 1244 (1992); K. Christensen and Z. Olami, Phys. Rev. A **46**, 1829 (1992); K. Christensen, Ph.D. thesis, University of Aarhus, 1992 (unpublished).
 - [10] S. Sinha and D. Biswas, Phys. Rev. Lett. **71**, 2010 (1993); S. Sinha, Phys. Rev. E **49**, 4832 (1994).
 - [11] P. Bak and K. Sneppen, Phys. Rev. Lett. **71**, 4083 (1993).
 - [12] J. Socolar, G. Grinstein, and C. Jayaprakash, Phys. Rev. E **47**, 2366 (1993).
 - [13] P. Grassberger, Phys. Rev. E **49**, 2436 (1994).
 - [14] Note that there is an ambiguity in this model. It often occurs that more than one site will have *exactly* the same height, as more than one site may topple to a height of exactly zero in a single avalanche. Two neighboring sites may then topple simultaneously; the above procedure does not define the result of such events. We have modified the rules in several ways, e.g., by adding a very small amount of random noise to ensure that no two sites have the same height, and they all give similar results.
 - [15] There is an explicit separation of time scales in the model. The slow time scale is the driving at unit rate. The avalanches occur instantaneously on this slow time scale.
 - [16] Y.-C. Zhang, Phys. Rev. Lett. **63**, 470 (1989); O. Narayan and A. A. Middleton, Phys. Rev. B **49**, 244 (1994).
 - [17] K. Y. Tsang, R. E. Mirollo, S. H. Strogatz, and K. Wiesenfeld, Physica (Amsterdam) **48D**, 102 (1991).
 - [18] The influence of inhomogeneity, which destroys the $1 - 4\alpha$ periodic state, is quite strong. Even a single defect, where $h = 0$ always, destroys the periodic state, and leads to a power-law distribution of avalanche sizes.
 - [19] C. S. Peskin, *Mathematical Aspects of Heart Physiology* (Courant Institute, NYU, New York, 1975); R. E. Mirollo and S. H. Strogatz, Siam J. Appl. Math. **50**, 1645 (1990).

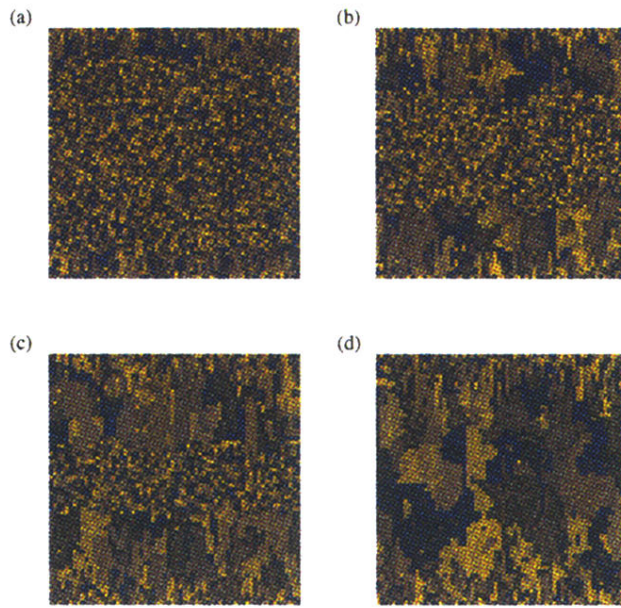


FIG. 1. Configurations of the Olami-Feder-Christensen model at various times after random initialization, demonstrating the invasion of the short-range correlated interior by the “SOC region.” The color corresponds to the height variables $0 \leq h_i < 1$. The boundaries are periodic in the vertical direction and open in the horizontal. The lattice consists of 64^2 sites, with $\alpha = 0.07$. Times are $t =$ (a) 1.2×10^3 , (b) 2.4×10^3 , (c) 6.0×10^3 , and (d) 36.0×10^3 .